SQU Journal for Science, 2021, 26(2), 107-125 DOI:10.53539/squjs.vol26iss2pp107-125
Sultan Qaboos University

Lithology Characteristics and Diagenesis of Late Pleistocene-Holocene Coastal Terraces of the Yemeni Red Sea: Implication for Paleoclimatic Records

Ahmed Saif Al-Mikhlafi*, Mohammed Abdullah Al-Wosabi, Ahmed Ali Alaydrus

Department of Earth Science, Faculty of Petroleum and Natural Sciences, Sana'a University, Sana'a, Yemen. *E-mail: ahmed.almikhlafi@fulbrightmail.org

ABSTRACT: The development of Holocene-Pleistocene fringing reefs in the Yemeni Red Sea (YRS) is controlled by sediment input and variations in accommodation space. Lithostratigraphic correlation of environmental facies in the investigated sites shows a sequence of successive events, and each can be subdivided into 2 or 3 main sequences. The upper sequence is characterized by the dominance of coral and coralline algal frameworks. The lower sequences are varied and can be attributed to spatial and temporal variability. Meteoric diagenesis is the most dominant and includes dissolution, calcrete, and coral recrystallization. Lithologic and mineralogic investigations of the Pleistocene-Holocene coral reefs display three aerial to subaerial diagenetic environments. These include freshwater-vadose, meteoric-marine-phreatic, and meteoric-phreatic zones represented at Al-Hajaja-Dhubab (Tr1), Perim (*Mayyun*) island (Tr2 and Tr3), and Kamaran island (Tr4) terraces. The effects of burial diagenesis increase progressively with depth, initially within the vadose zone and, ultimately, into the underlying phreatic zone. The phenomenon of dolomitization and siderisation processes are also occurring in the sections that exhibit brine and freshwater interaction with the iron-rich basaltic rocks. Climatic variation during interglacial-glacial cycles and the wind systems that prevailed in the area have contributed largely to the final deposition. The transition from interglacial to glacial climates in Arabia was characterized by higher effective rainfall, accompanied by aeolianite dissolution and karstification.

Keywords: Climatic variations; Aeolianite; Diagenesis; Terraces; Red Sea.

الخواص الصخرية والتغيرات المابعدية للشرفات المرجانية لعهدي البليستوسين المتأخر والهولوسين في الجانب اليمني للبحر الأحمر: تضمينها كسجل للمناخ القديم للأرض

أحمد سيف المخلافي، محمد عبدالله الوصابي وأحمد علي العيدروس

الملخص: نمو الشعاب المرجانية الحاجزية في عهدي البليستوسين والهولوسين في الجانب اليمني من البحر الأحمر يتحكم فيها كمية الرواسب المنقولة والفراغ المكاني. تظهر المقارنة الصخرية وطباقية المقاطع المختلفة سلسلة من الأحداث المتتابعة، ويتميز كل موقع بصفات تميزه عن الآخر. يتميز التتابع العلوي بسحنات غنيه بأحافير المراجين والطحالب المرجانية بينما يتنوع التتابع الأسفل ويختلف من مكان لآخر تبعا للتغيرات الزمانية والمكانية. تعتبر المياه الجوية هي المسؤولة عن التغيرات المابعدية لهياكل الشعاب المرجانية والتي تشمل عمليات الإذابة، اعادة التبلور وتكوين طبقة الكالكريت. الفحص الصخري والمعدني للشرفات المرجانية أظهرت ثلاثة أنواع من التغيرات السطحية والتحت سطحية مرتبطة بتفاعل الماء مع الشعاب المرجانية لتشمل مياه عذبه إرتشاحية – مياه جوية- مياه بحر- مياه جوفية؛ ومياه جوية – جوفية لتمثل على التوالي شرفات منطقة الحجاجة (ذوباب)، جزيرة بريم (ميون) وجزيرة كمران. تزداد التغيرات المابعدية مع العمق في بداية منطقة الفادوز وتسنمر في الأسفل الى نطاق الإرتشاح. يُفسِّر ظهور معادن الدولوميت والسيدرايت في هياكل بعض الكائنات المرجانية حدوث التبادل الأيوني بينها وبين المياه شديدة الملوحة والمياه العذبة مع الصخور البازلتية الغنية بالحديد. ساعدت التغيرات المناخية اثنا الدورات الجليدية وبين الجليدية وما صاحبها من فترات مطيرة وهبوب للرياح على تكوين طبقة الكالكريت على أسطح هذه الشرفات.

الكلمات المفتاحية: التغيرات المناخية، عمل الرياح، التغيرات المابعدية، الشرفات المرجانية

1. Introduction

Emerged Pleistocene coral reef terraces form a prominent landform in the central and northern Red Sea coast. However, southern Red Sea coasts are devoid of these prominent structures and the Pleistocene terraces are mainly restricted to island fringing reef or some buried ill-formed terraces. Yemen dominates the southwestern part of the Arabian Peninsula and occupies the longest coast of the southern Red Sea known as the Tihamah Plain. The coastal plain of Tihamah is a flat sandy coastal plain 30-60 km wide and 415 km long, stretching from Bab al-Mandab in the south to the Saudi Arabian border to the north. The Yemeni Red Sea (YRS) coast is bounded by the great escarpment, which rises abruptly from an altitude of ~200 m to >3000 m above sea level [1]. The escarpment marks the uplift of the margins of the Arabian and African shields and is the structural edge of the Red Sea rift area [2].

Erosion of the hinterland bedrock has supplied terrigenous sediment to the coast and shelf via monsoon wind systems. Because the shelf is relatively wide in the YRS, it is likely to facilitate the deposition of sediments in shallow water to hinder coral growth [3]. The Pleistocene fringing coral reefs in YRS are typically limited to a maximum depth of 3-4 m [3], which can be worked as excellent sea-level indicators [4]. Consistent with [5], the Pleistocene reef types of the YRS can be classified into (i) mainland fringing reefs, (ii) island fringing reefs, and (iii) submerged patch reefs, of which (i) and (ii) are discussed here. Correlation and dating of emerged Pleistocene reef terraces along the Red Sea coast have the potential to enhance the understanding of the tectonic, palaeogeographic, and palaeoclimatic history of the region, as well as to reconstruct sea-level changes during the Pleistocene [6].

Diagenesis is a ubiquitous phenomenon of Pleistocene corals along the Red Sea coasts [7-12]. Diagenetic changes of coral skeletons involve the meteoric transformation of coral skeletons biogenic aragonite to non-biogenic calcite at vadose or phreatic zones. Diagenesis can be listed as (i) dissolution of primary coral aragonite, (ii) infilling of skeletal pore spaces with secondary carbonate cement and/or microbialites [13-16], and cavity filling mud [17], (iii) recrystallization of coral aragonite to calcite [16]. Diagenetic transformations also occur in living reef corals [16], [18-22]. Carbonate recrystallization is typically associated with crystal growth and transformations of metastable Mg-calcite and aragonite to calcite in meteoric and burial diagenetic environments (e. g., [23-25]).

Being a prominent feature, several studies have been conducted to investigate the lithostratigraphy and evolution of the Pleistocene terraces along the coast, northern Red Sea (Aqaba area) [7], [11], [26] and references therein), central Red Sea (Saudi Arabia and Sudan) [6], [27-29] and Farasan Island [30-32] and Dahlak Reef in the southern Red Sea in Eritrea [33], [34]. However, most studies carried out in the YRS pertain to the biodiversity of corals and biogenic reefs [3], [5], [35-36]. This study is aimed to investigate the lithology and diagenesis of carbonate terraces based on field observations and X-Ray Diffraction analyses of a series of aerial and subaerial Pleistocene reefs of YRS. The main purpose is to describe the composition and texture and to document the diagenetic history of the sediments. The calcrete deposit developed atop of Pleistocene terraces will be described to identify the likely hydrologic and palaeoclimatic conditions associated with periods of calcrete deposits.

Climate oscillation during the Pleistocene time was accompanied by cyclic deposition of aeolianites across the Red Sea; similar to other deposits in a range of locations worldwide; e.g southern Australia [37-43], the Bahama Islands [44]; and South Africa [45-46]. In the Red Sea, the aeolian terrigenous material is assigned to the deserts of Northern Africa and/or is from the Arabian Peninsula [47-54]. The sea-level rise following the onset of deglaciation generated a rapid flush of detrital material that accumulated on the continental margins and the previously emerged zones of the Bab-el-Mandeb area [55]. Two cores retrieved from the Gulf of Aden and the central Red Sea show that the grain size of aeolian dust records have lower median values during the peak interglacial periods, to indicate slow weathering and erosion corresponding to high vegetation cover [56] and references therein.

The objectives of this study are to: (i) provide a lithological description of the Pleistocene reef terraces from YRS coasts; (ii) study freshwater diagenesis of the vadose and phreatic zones, and reconstruct the diagenetic environments by the characterization of the mineral composition of coral skeletons; and (iii) study the development of calcrete deposits atop of marine terraces, which can provide a record of the paleohydrological pattern in southern Arabia.

2. Geology and physiography of the study area

The investigated sites in this study include Al-Hajaja (Dhubab) terrace (Tr1), Perim Island terraces (Tr2, Tr3) (Figures 1a and b) and Kamaran Island terrace (Tr4) (Figure 1c). In addition, patch corals of Holocene age are found intermixed with siliciclastic deposits in Om Gedi (OG) and Ras Harafa (RH) terraces (Figure 1 c). All the terraces are designated as of Pleistocene age and belong to Kamaran members of the Abbas Formation [57].

The first-order control of the arrangement and orientation of shallow-water coral reef environments in the Red Sea is explained by rift-related tectonics and both attached and detached reef systems orient along the direction of the main Red Sea rift axis [58]. The volcanic activity occurring along the Red Sea runs in a roughly northwest-southeast line, and the islands appear above the sea surface, rising from a shield volcano.

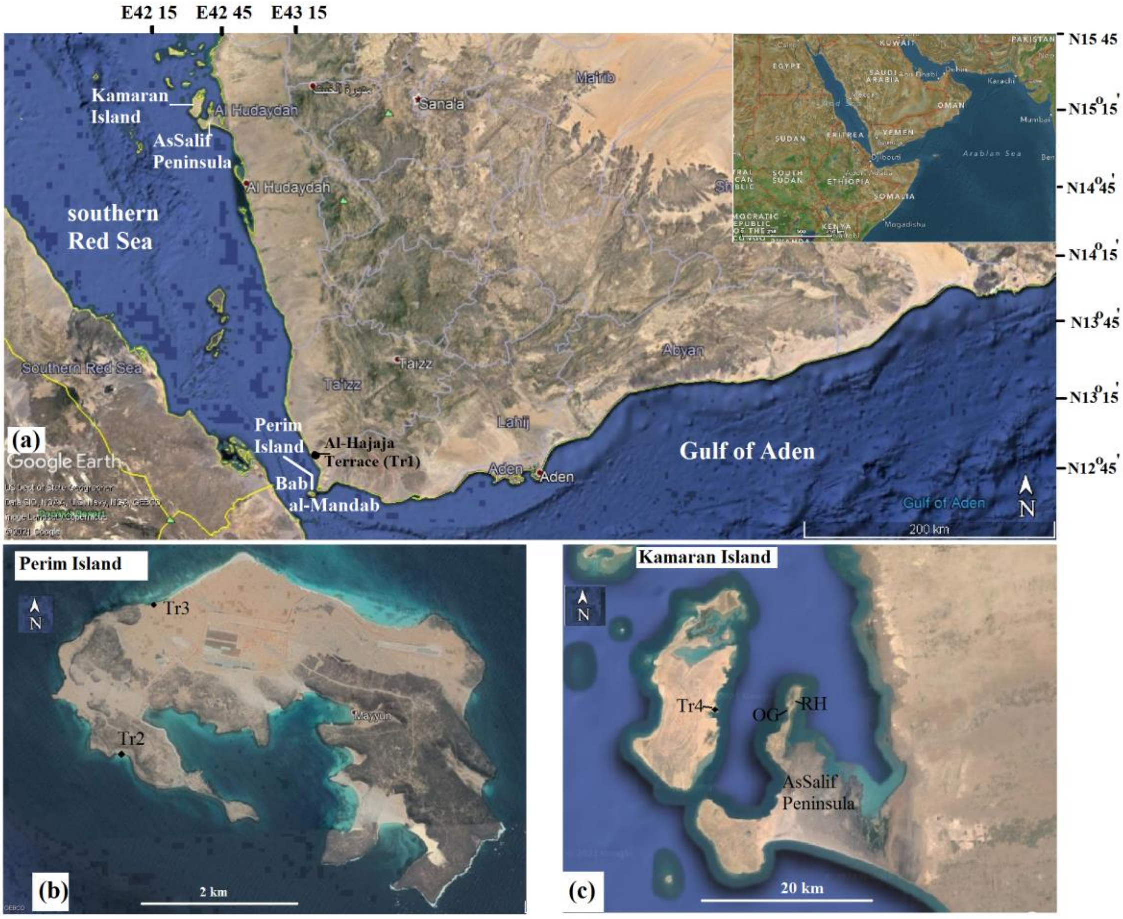

Figure 1. (a) Satellite photos of Yemen territory superimposed by a regional map showing study locations from the southern Red Sea, Al-Hajaja-Dhubab location (Tr1), Perim and Kamaran islands; (b) Perim Island terraces (Tr2) and (Tr3); (c) Kamaran island terrace (Tr4). Corals of Holocene age are also shown in Ras Harafa, (RH), and Om Gedi (OG) terraces.

The narrowness of Pleistocene reef terraces at YRS coasts is attributed to: (i) shallow and wide continental shelves that entrapped sediments within the reefs to create a substrate instability, accompanied by turbidity, restricting coral reefs to develop into fringing reefs [58-60]; (ii) the growth of the reef in the Red Sea is tectonically controlled by the Red Sea rift [61-63], and the southern Red Sea is tectonically stable ([64] and references therein); (iii) large siliciclastic input from the hinterland correspond with pluvial periods of Arabia, and reefs are typically absent in wadi mouths [36], [65], but their presence cannot be abandoned [61], [66]. The large siliciclastic input appears to be associated with a marked increase in turbidity that impedes the reef growth. This is valid even if conditions are suitable for the growth of corals; the continuous deposition of sediments would cover the growing corals leading to their smothering and death

3. Materials and methods

Hand specimens and *in situ* outcrop descriptions were carried out for terraces to study the physical characteristics and rock lithology. Mineralogical investigations were performed on skeletons of fossil corals from the emerged Pleistocene reef terraces in Bab al-Mandab (PI and Al-Haj coast), and Kamaran Island in the Yemeni Red Sea. These corals were subjected to XRD analyses at the Earth and Environmental Sciences Department, University of Minnesota, to appraise the diagenetic changes for the corals during the occurrence. Samples were ultrasonically cleaned, and then approximately 100 to 200 mg of material was ground under ethanol to less than 50 µm grain size and smeared onto a glass slide. The crushed skeletal material from each sample was mounted on a low background holder using the Cu Kα radiation to record the XRD patterns. The scanning was run in 2θ ranging from 5° to 55°. XRD patterns of skeletal material were compared to the XRD peaks for Inorganic Crystal Structure Database aragonite and calcite standards. Bulk mineralogy of coral skeletons was verified by powder XRD using a Rigaku Instrument, and the percent of aragonite and calcite in each sample was calculated using JADE 7 software. The relative amounts of aragonite, calcite, and dolomite were determined through measurement of X-ray peak-height intensity ratio of the aragonite d (111) peak, calcite d (104) peak, and dolomite d (104) peak. The content of calcite was quantified as the ratio between peak intensities at 26.2θ (aragonite), and 29.4-29.5θ (calcite). The calcite detection limit was determined to be 1% by measuring mixtures of aragonite and calcite powders with known calcite to aragonite ratios. The ratio percentages were prepared by selecting a pure aragonite end-member from the modern coral specimen (*Acropora* sp.), collected from As-Salif Peninsula. Similarly, a pure calcite end member was prepared from a sample collected at Kamaran Island. Each sample was ground separately in an agate mortar under ethanol to less than 50 μm grain size and subsequently mixed at relative proportion to make a series of XRD standards. Slides for XRD detection were prepared by mounting the well-mixed standard powder on microscopic glass covers. These ratios were compared with a standard calibration curve prepared with various calcite concentrations (0%, 1%, 5 %, 25 %, and 100 %) weight percentage, calcite in aragonite, and were routinely measured (Figure 2).

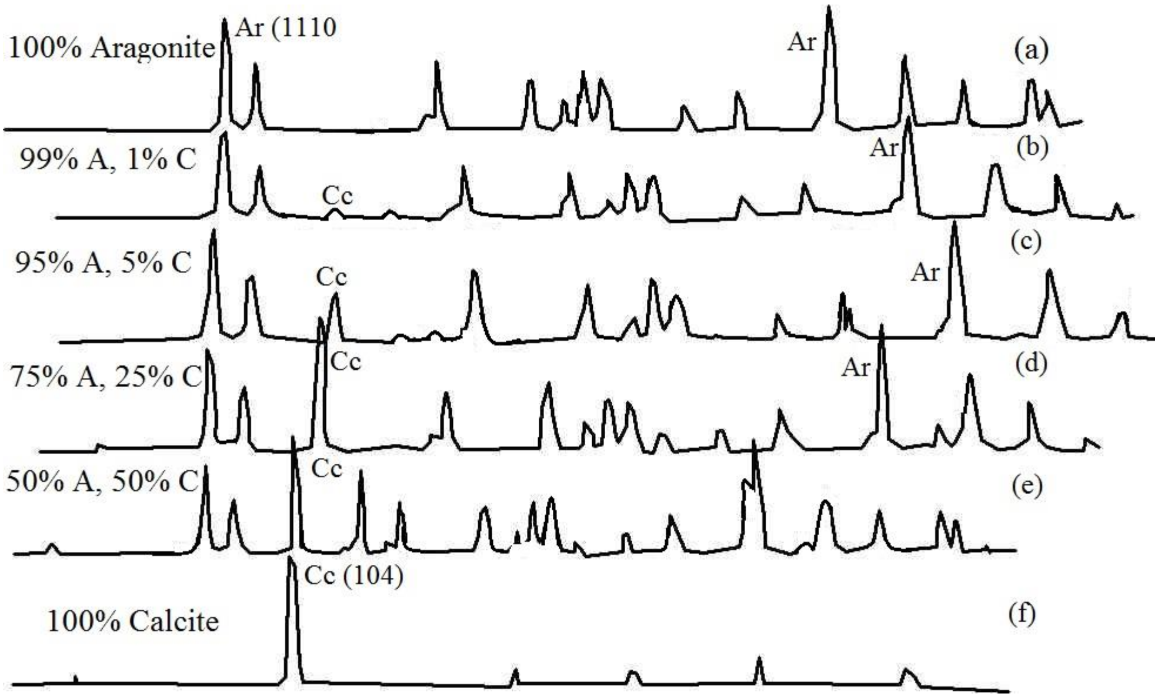

Figure 2. Different percentages (%) of calcite and aragonite in the studied samples, from (a) to (f), the percent of aragonite is decreasing from 100% to 0% while calcite is increasing from 0 to 100%.

4. Results

4.1 Stratigraphy and Lithofacies

4.1.1 Holocene terraces

The coastal plain of the Yemeni Red Sea is a large alluvial plain composed of siliciclastic deposits. The plain has been built out quite rapidly as shown by ^{14}C dating of Neolithic coastal middens near Wadi Rima, 55 km SSE of Al Hudaydah. These middens have been dated as 8,084 to 8,480 years BP and are now >10 km inland [67-68].

Holocene fringing reef development around As Salif Peninsula is controlled by variation in accommodation space (as a function of sea-level and antecedent topography) and sediment input. The Holocene accretion is limited to sparse patches or solitary corals, and no Holocene emergent terraces are present. Modern patch corals of *Acropora* sp. and *Porites* sp. intercalated with siliciclastic sediments have been spotted atop of the As Salif salt diaper, Om Gedi, and Ras Harafa north of As-Salif Peninsula [12] (Figure 3). $^{230}Th/U$ dating of corals from As Salif Peninsula yields to mid-Holocene age [12].

Figure 3. Patch coral reefs of Holocene age in As Salif peninsula dated by [12]. (a) Corals atop of salt diaper, (b) Om Gedi corals of *Acropora* sp. type intermix with siliciclastic sediments, (c) Ras Harafa corals covered by gypsum (sabkha).

The main reason for the lack of reef development is the introduction of large amounts of siliciclastic sediments from the Tihama Plain by the action of monsoon winds instigated by the Indian Ocean monsoon.

4.1.2 Pleistocene terraces

Based on their lithology, the biofacies of this study are variably susceptible to changes in sedimentation patterns, sea-level fluctuation, and climatic changes. Several distinct biofacies can be recognized including the major growth framework. The coral growth framework facies comprise branching and massive coral forms in growth position, usually encrusted by coralline algal veneers. Detrital facies include skeletal rubble and carbonate sand facies. The rubble facies is composed mostly of a mixture of unsorted, angular to rounded, gravelly fragments of corals, bivalves, foraminifera, and calcareous algae. Pleistocene terraces display a wide range of calcretization from incipient calcrete, which appears as chalky micritic lumps, sporadically dispersed within the host sediments through nodular calcrete to a well-developed subaerial massive calcrete zone which caps the terrace.

4.1.2.1 Al-Hajaja (Dhubab) reef section

The Al-Hajaja terrace (Tr1) is the mainland fringing reef of the last interglacial period that receives appreciable amounts of siliciclastic sediments as aeolian dust and/or fluvial/alluvial material from adjacent terrestrial mountains (Figure 1). The terrace belongs to shallow-marine reef environments raised to + 4 masl by a relative fall in sea level [4]. The reef front drops gradually from ~ + 4 masl at the surface to a sandy flat of ~ +1 masl. The terrace was buried under sediments and was exposed due to road excavation, which may suggest that the late Pleistocene terraces have been buried under the alluvial fans formed later in a sequence of wet and dry periods in southern Arabia.

Road material excavation through the reef terrace has revealed three types of coral zonation that develop from the base up to the crest. At the base, the terrace is composed of massive coral species *Platygyra* sp., grading into a mixed zone dominated by *G. fasicularis*, *Stylophora* sp., *Goniastrea* sp., and *Acropora* sp. and *Faviids* sp at the top. The *Acropora* zone is displayed as broken branches. Corals are discontinuous and may be missing entirely along the crest of the individual terrace. Two distinct facies can be distinguished, lower and upper.

Lower Reef Unit: The lower tracts of the Al-Hajaja section are formed of solitary massive corals, surrounded by hardground pedogenic carbonate which displays large calcrete mottles. It is a regression that receives a significant amount of alluvial/aeolian terrestrial material, especially during the wet seasons, contributing to the mottles formation (Figure 4 (A)). Spots of carbonate/halite structure are observed in the lower section, which shows that a dry climate prevails in the area (Figure 4 (A)). The whole unit has sabkha characteristics.

Upper Reef Unit: The terrace is composed of colonial corals that exhibit a variety of morphotypes such as branching (*Acropora* sp. and *Porites* sp.), and massive types (*Faviids* sp., *Platygyra* sp., *G. fascicularis*). Reef-building corals are the dominant assemblages in the Al-Hajaja terrace, and the *Galaxea fascicularise* are the dominant coral species, consistent with modern reefs as described by [35] (Figure 4 (B)). The biofacies of the terrace are shown in the stratigraphic log (Figure 4 (C)).

Calcrete deposits have developed at the top of Al-Hajaja terrace and range from a hard, massive calcrete zone at the top of the terrace to a transitional mottled calcrete horizon below (Figure 4 (B-a)). A dense laminated crust produced at the top of the terrace suggests fluvial/ alluvial inputs and carbonate redistribution (Figure 4(B-b,c)). Another sign of calcrete deposits is the occurrence of rootcretes to indicate carbonate deposition and redistribution (Figure 4 (B-d)).

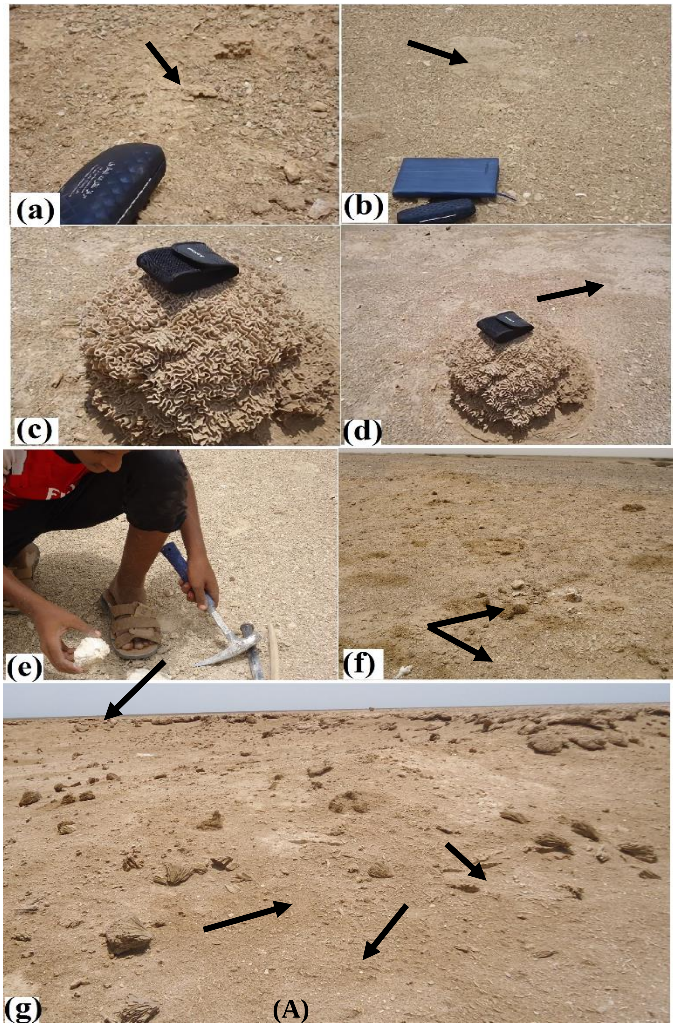

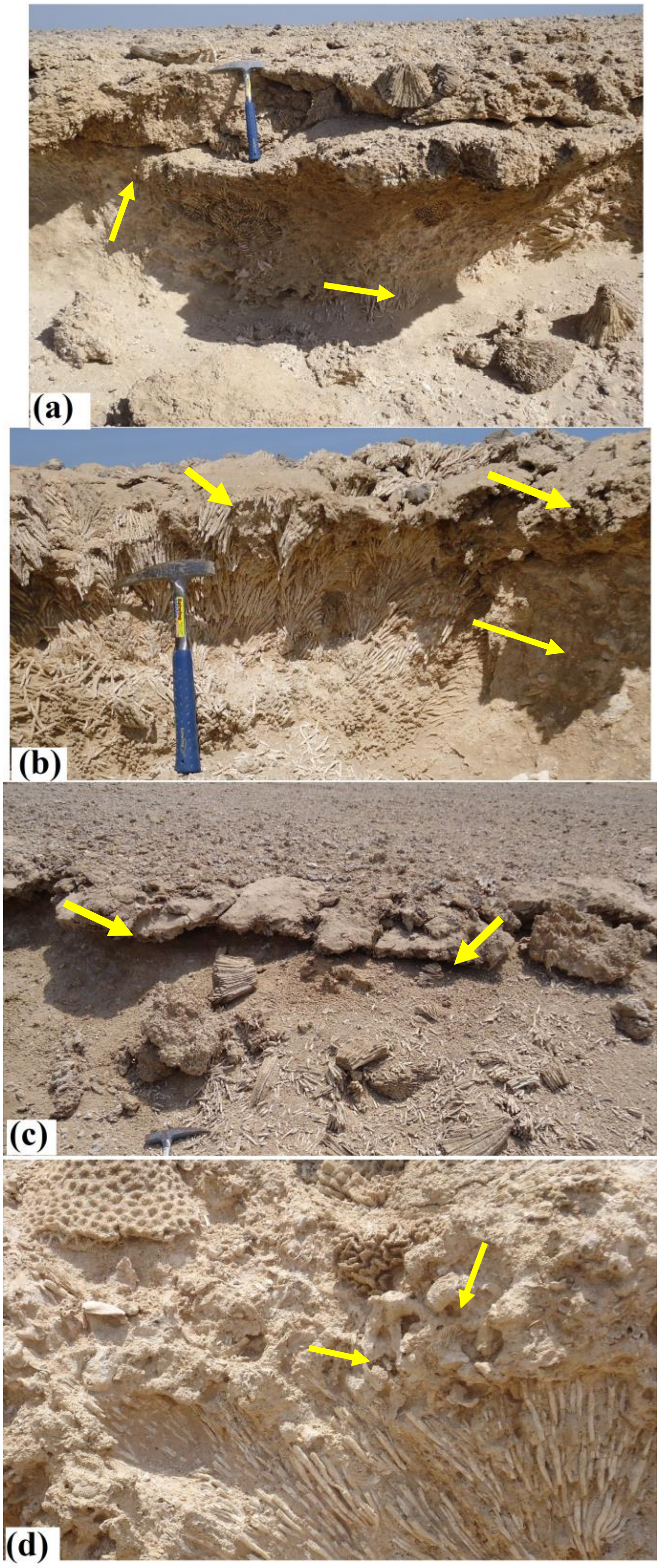

(B)

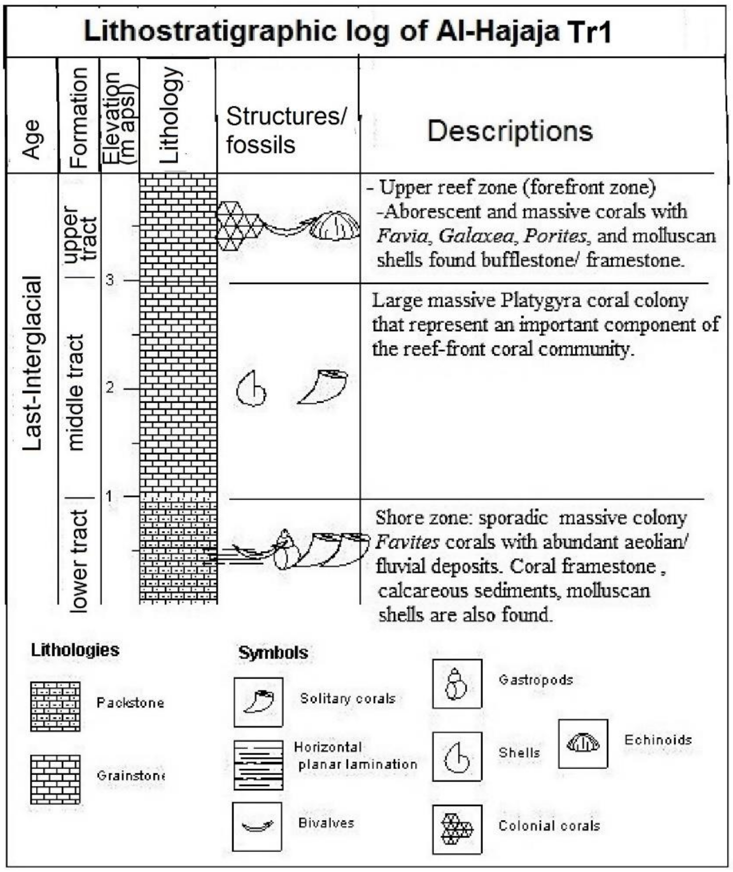

(C)

Figure 4. (A) Lower reef unit of Al-Hajaja terrace (Tr1): (a) grains coated by pedogenic carbonate during calcretization; (b), (c), and (d) are thin micritic filaments coating coral predecessor, which display as large carbonate/halite mottles (arrows); (c) and (d) corals encircled with carbonate/halite mottles; (e) fossil coral of Last Interglacial age showing chalky appearance and complete alteration into calcite; (f) and (g) Sabkha like structure with white mottles, corals/shells fragments scattered in the area. (B) Field photographs of the upper reef unit of the Al-Hajaja terrace showing coral buffelstone and wackestone formations. (a) A hard and massive calcrete is developed in the top relative to more friable material at the base; the yellow arrow points to the disconformable contact; (b) terrestrial deposits develop a dense laminated crust overlying coralline reef at the top and a transitional mottled calcrete horizon below (arrow); (c) lamination at the top of the terrace, scattered fossils lower; (d) Coral buffelstone with pseudo-rhizocrete developed on the top. (C) Stratigraphic log of Al-Hajaja section.

4.1.2.2 Perim (Mayyun) section

Two Pleistocene coral reef terraces have been investigated in Perim Island, namely coral dominant (Tr2) and rubble-dominant reef-flats (Tr3) (Figure 1). Important for the geomorphology of reefal terraces in PI are monsoonal wind reef patterns induced by the Indian Ocean Monsoon. The climate in the Bab al Mandab is subtropical and varies significantly during the seasons. The Perim Island terrace (Tr2) is a wave-cut coral-reef terrace that emerged at the SW side of PI, facing the deep channel of the Bab al-Mandab strait. The terrace is lined by SW monsoon wind direction and represents a remnant of the reef flat. The effective tidal range at Tr2 is ~ 2 m [69], consistent with strong wave action, and the development of the terrace formation is very much related to the wave direction. The terrace (Tr2) (Figure 5 (A)) is composed of marine sequences and consists of an association of shallow marine grain supported carbonate and coralline boundstone facies residing above lag deposits (Figure 5(A)). The successive facies of Tr2 show in the lithostratigraphic log (Figure 5 (B)).

Based on the macroscopic inspection, three Pleistocene facies may be distinguished (Figure 5 (A)). The gravel material that formed at the base represents lag deposits brought from the hinterland during the marine regression.

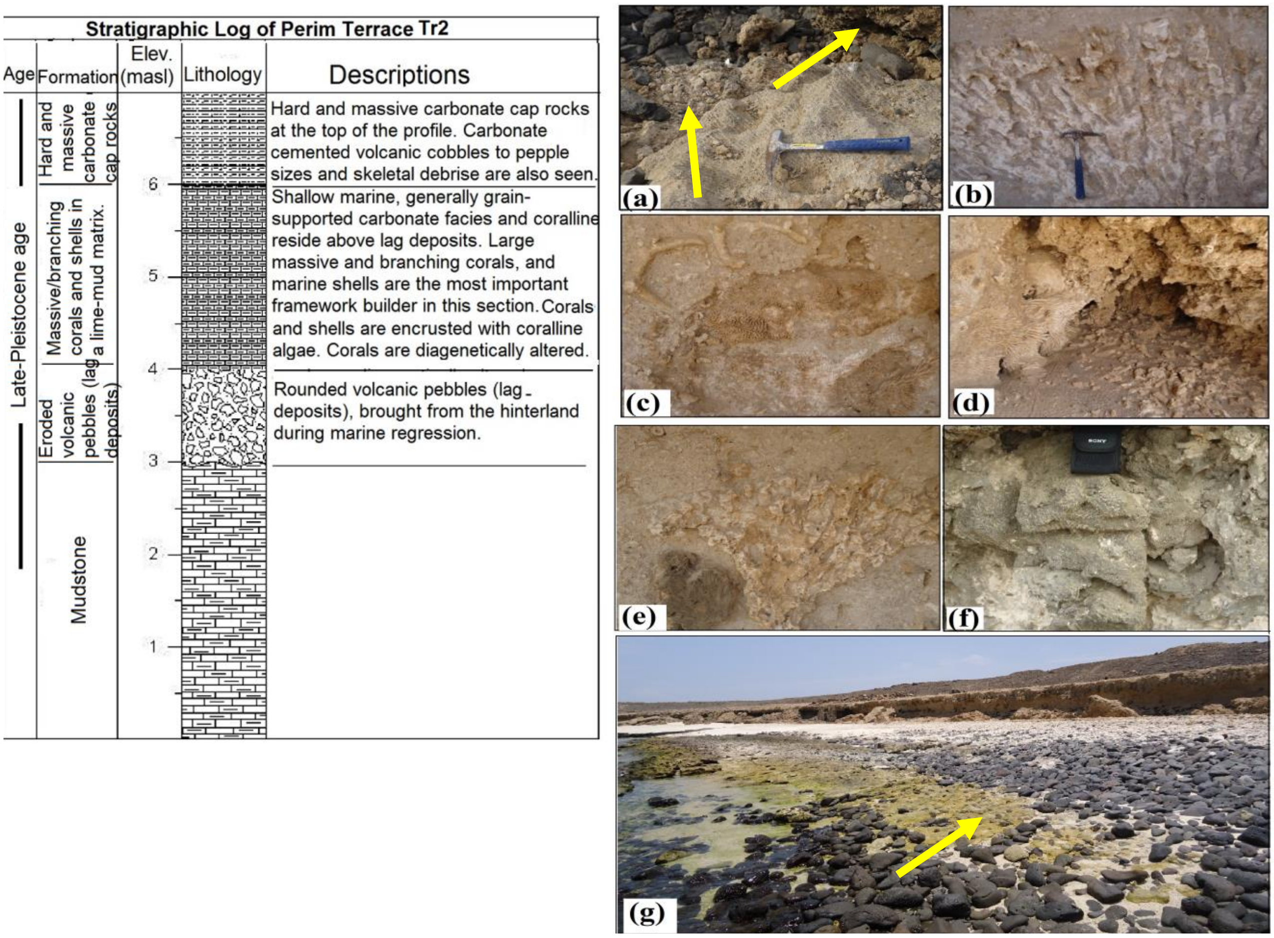

(B)

Figure 5. (A) Excerpts from Perim Island terrace (Tr2); (a) Concretionary calcrete with coalescent nodules (yellow arrows); (b-e) large (neomorphic skeleton) branched corals embedded in coralline algae; chalky appearance is common throughout the sections; (f) coral fragments smeared by laminar carbonate; (g) Field view of the Tr2 showing the lag deposits overlain by carbonate deposits, note the hard nodule calcrete tops less friable deposits (yellow arrow). (B) Lithostratigraphic log of Tr2.

Coralline boundstone facies consist of isolated patch massive and branched corals in both growth and non-growth position typical of reef flat formed in a poorly sorted skeletal wackestone and packstone matrix. Large branched corals of *Porites* type is the most important framework builder in this section. The chalky appearance of these corals represents relicts of the original skeletons that were preserved in the neomorphic calcite form. The skeletal debris that overlies the uppermost facies may form another phase of sea level advance in which skeletal debris is deposited upon the reef flat.

A leeward fringing reef (Tr3) formed predominantly of coral rubble faces the shallow channel of the Bab al-Mandab and is developed to the north of Perim Island (Figure 1). Mollusk shell pieces and echinoid remains are also found (Figure 6 (A)).

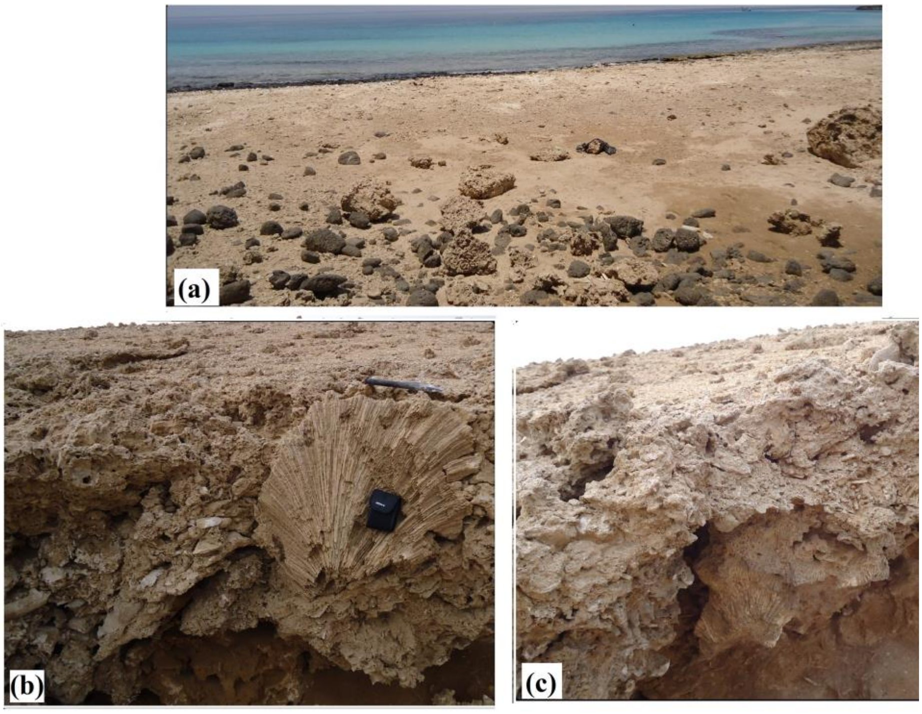

(A)

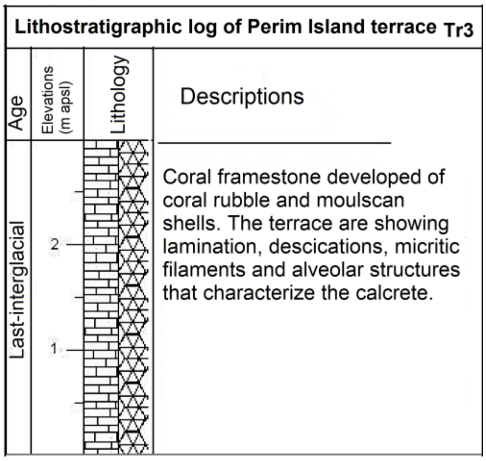

(B)

Figure 6. (A) View of rubble reef-flat of northern PI (Tr3) of ~1.5 km length and 2 km width, probably developed coinciding with the SE monsoon wind prevailing in Arabia; (b and c) show lamination, desiccations, micritic filaments and alveolar structures that characterize the calcrete. Note the solution caves and cavities. (B) Stratigraphic log of Tr3 terrace.

The rubble that forms the terrace is derived from windward reef front below mean low water (SE monsoons) formed of dead corals broken on the reef front, accumulates in situ, and is picked up and transported up into the rubble flat. The intensity and frequency of these processes are functions of wind strength, sea state, and tidal condition [70].

4.1.2.3 Kamaran Island (KI) Tr4

The stratigraphic unit of KI members is essentially made up of coral reef limestone, mainly of scleractinian corals, coralline algae, gastropods, and bivalves, and form *framestones*, similar to what is exposed at Farasan Island [71] (Figure 7 (A)). Diagenetically altered carbonate mud, cryptocrystalline carbonate matrix, or microcrystalline micrite grains also form a significant part of Kamaran members, reflecting a low energy and low current activity environment [72]. Recent deposits composed of pure calcareous sands, gravels, and shell fragments are found above the Kamaran member. The lithostratigraphic sequence (Figure 7 (B)) is after [62].

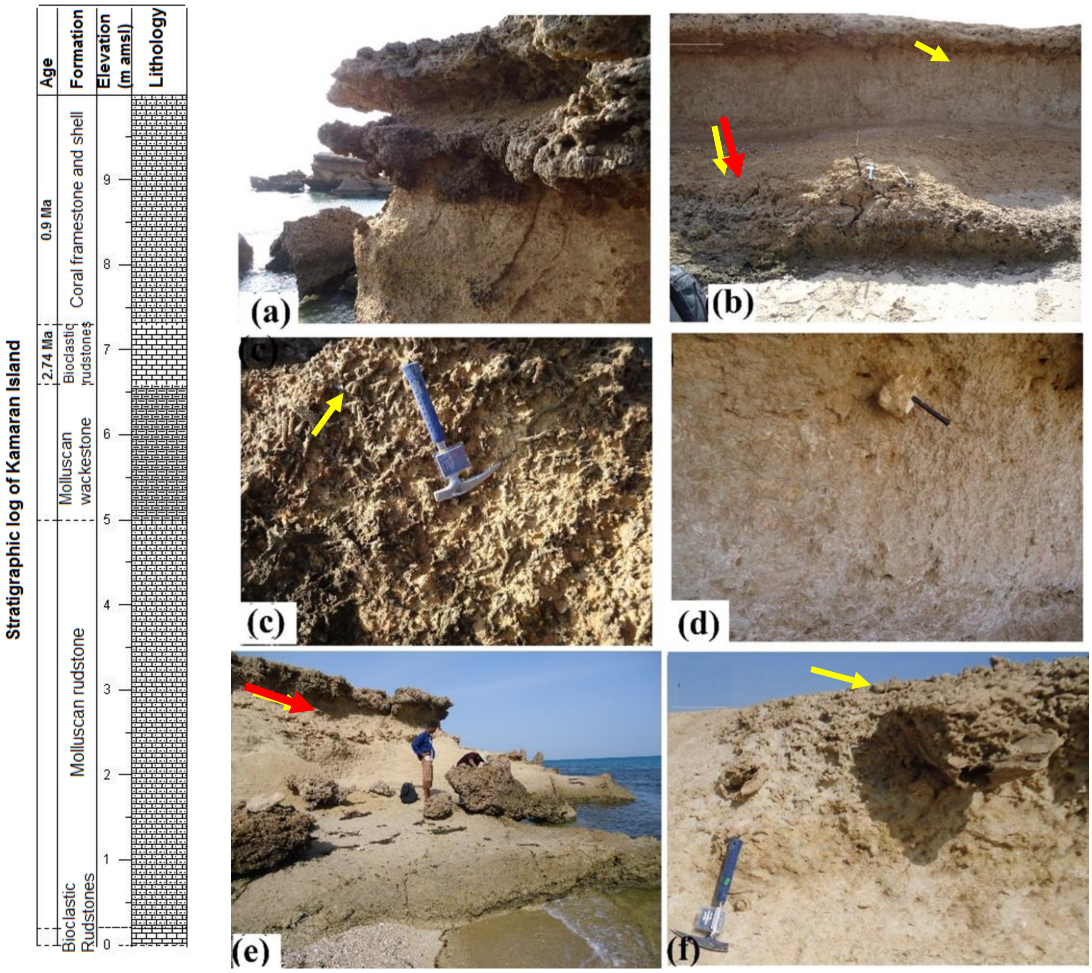

(A) (B)

Figure 7. (A). Kamaran terrace developed calcrete zone; (a) highly altered reefal limestone overlies marly limestone; (b) field view of thick, mainly hard and massive cap rock at the top of the profile, overlying slightly friable and chalky carbonate at the base (yellow arrows); the lower platform is a cluster of root cast often found exposed on aeolian sand-dunes (red arrows); (c) cluster roots sediments; field view of irregular coral mold fragments embedded in Pleistocene carbonate and displayed as rhizoliths; (d) incipient massive calcrete and nodular calcrete; (e) terrace with highly altered Pleistocene fossil corals at the top surface; coalesced nodules of calcrete display at the middle; (f) calcrete casts and molds of fossil roots can be seen in this outcrop of known limestone; cluster root sediments calcretization of root burrow infill and development of pseudo-rhizocrete and pseudobreccia. (B) the lithostratigraphic section after [62].

The most altered coral samples were recorded in Kamaran terraces, suggesting their being of the early Pleistocene [62]. Being the oldest, the mineralogy of Kamaran terraces shows coral skeleton predominated by high-magnesium-calcite.

A series of calcrete deposits were developed along the Kamaran terraces to suggest active terrestrial inputs from the mainland. The caprock of the Kamaran is formed of calcrete deposits and consists of hard and massive cap rock which overlies slightly friable and chalky carbonate at the base (Figure 7(A)). A cluster of irregular coral mold fragments is embedded in Pleistocene carbonate and displayed as rhizoliths (Figure 7(A-c)). Calcrete casts and molds of fossil roots displayed at the top surface (Figure 7 (A-f)) are often found exposed in aeolian sand dunes. Root casts are developed, in which the central channel of the cast may be void or filled with soft carbonate [73]. Micro-organisms, bacteria, blue-green algae and fungi, and root respiration, in addition to root symbioses, play a major role in the formation of root casts [73-74].

4.3 Mineralogy

Mineral identification of fossil corals was scrutinized following [75]. XRD analysis of modern corals from As Salif Peninsula shows skeletons of *Acropora* and *Porites* corals are predominantly composed of aragonite, with no evidence of calcite or dolomite present (Figure 8a).

Correspondingly, the majority of Late-Pleistocene corals from Al-Hajaja terrace show that corals from the upper unit have overall pristine coral skeletons. XRD analysis shows that aerial massive corals display fair preservation, with only traces ~2-3 % of calcite present (Figure 8b and c). However, the same species of massive corals collected from the lower tract at an elevation of ~2 to 1 masl yielded a mixed mineral structure that includes aragonite, calcite, and dolomite (Figure 8d), and complete skeletal neomorph transforms into calcite and dolomite. Some traces of aragonite also remain (Figure 8e) to suggest dolomitization with depth.

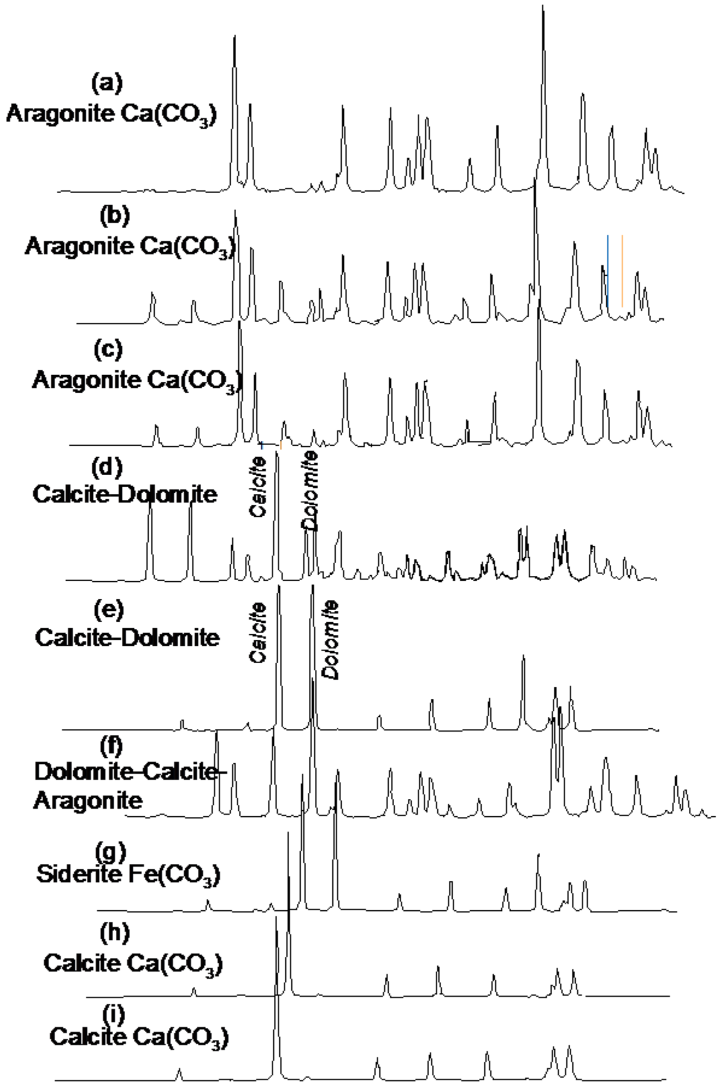

Figure 8. XRD analysis of coral samples from YRS. (a) modern corals from AsSalif Peninsula; (b), (c) and (d) fossil corals from Al-Hajaja; (f), (g), (h) fossil corals from Perim Island; (i) fossil corals from Kamaran Island.

The majority of the corals from PI are diagenetically altered. The intense alteration can be judged from the strong calcite peaks and dolomite minerals that appeared in the XRD graphs.

Coral diagenesis in the PI terrace involves replacement by diagenetic minerals such as siderite and calcite of the original biogenic composition. XRD analyses of corals from Tr2 show peaks displaying multiple mineralogical compositions that include an aragonite-calcite-dolomite mixture (Figure 8f), calcite-siderite (Figure 8g), and pure calcite (Fig.8h), to suggest prolonged interaction of saline-meteoric-corals at the phreatic zone.

Fossil corals from KI show complete alteration into calcite, and all the XRD peaks show the main calcite to stand at nearly the right position of calcite peaks *d* (104) with no shift in peak position (Figure 8i).

5. Discussion

5.1 Holocene corals

The lithologic and stratigraphic investigations of recent sediments on the coasts of the southern Red Sea show that the two major facies developed in the area are carbonate deposits ~3m thick, overlaid by siliciclastic deposits [76].

Holocene corals are poorly developed in the area and their presence is restricted to patchy corals. This can be attributed to the absence of accommodation space needed for coral growth due to the large terrestrial inputs.

The Holocene coral reefs are developed antecedently on the Pleistocene corals that work as Holocene fringing reef pedestals ([65], [77] and references therein).

Corals of the Holocene age have an aragonite skeleton, and show U depletion. The U depletion may reflect the influence of the Holocene pluvial period that prevailed in Arabia during the Holocene [78], [79].

5.2 Pleistocene coral reef terraces

The scarcity of Pleistocene coral framework terraces in the southern Red Sea is linked to a continuous supply of siliciclastic material from the high mountains that flank the Tihamah Plain. The present-day climate in the southern Red Sea is arid to hyper-arid with evaporation rate far exceeding rainfall rate throughout the year, and does not support large siliciclastic inputs. However, Holocene and Pleistocene pluvial periods in southern Arabia were characterized by heavy rainfall and stalagmite growth in southern Arabia [79], [80], [81], [82], [83] diminishing the formation of a classic reef [36].

Diagenesis is widespread in the Pleistocene terraces, and the intensity of diagenesis is sporadic, showing temporal and spatial changes. Coral diagenesis involves replacement by diagenetic minerals, such as siderite and calcite, of the original biogenic composition. XRD analysis of corals from Tr1 shows dolomitization for samples in the lower section of the terrace, to suggest prolonged interaction of saline-meteoric-corals at the phreatic zone. The majority of corals from Tr2 are diagenetically altered and their skeletons are recrystallized and entirely replaced with calcite. The coral skeletons show a broad range of complex mineral structures, which are from a dolomite-aragonite-calcite mixture, calcite-dolomite to pure calcite and siderite. As a flat reef terrace, Tr2 is susceptible to receiving meteoric ground waters via sheet-water-like forms in the coastal-saltwater mixing zone, suggesting prolonged interaction of freshwater and corals at the vadose/phreatic zone.

Dolomitization is not uncommon for corals in the mixed meteoric/marine zone that lies between the phreatic marine and phreatic pore water zone [84], [85]. According to [86], meteoric diagenesis is more sporadic, and coral skeletons from the same terrace display a broader range of preservation from apparently pristine to completely altered. Vadose fluids percolating coral reefs change the dense aragonite of corals to a white “chalky” carbonate, and such chalkification starts in the center of the coral branch, and with the passage of more vadose fluids moves towards the periphery [87].

The mechanism suggested for the dolomitization processes is seepage reflux in which the dense hypersaline brines seep into the subsurface [24], [88], [89].

Siderite is one of the main diagenetic constituents which affected siliciclastic sediments immediately after deposition [90]. The environmental conditions under which siderite is developed are suboxic conditions with a relatively low concentration of organic matter close to the sediment-water interface, and a low accumulation rate [91], [92]. As a result, siderite ($FeCO_3$) occurs widely in sedimentary environments and is used as a measure of a reduction state in the environment of deposition [90], [91], [93], [94]. The presence of siderite, therefore, indicates that iron supply exceeds sulfide supply [95]. For siderite changes to form in the PI section, the source of iron is from the alteration of basaltic rocks in the catchment area in freshwater environments.

Calcrete is ubiquitous and occurs in a variety of forms in all of the studied Late Pleistocene terraces of YRS ranging from incipient, nodular, to concretionary and massive calcrete. Calcrete is interpreted to be pedogenic and related to the diagenetic alteration of host carbonate deposits in the vadose zone during subaerial exposure.

The thickness of the calcrete differs in composition at KI compared to PI and Al-Hajaja terrace. It is more developed in KI (early Pleistocene), but less developed in Al-Hajaja mainland terrace (Late Pleistocene), which can be attributed to the length of exposure. Old terraces have been exposed to further calcretization during relatively successive wet periods. In the calcretization zone, dissolution of carbonate skeletons and reprecipitation of calcite cement are common, and neomorphic transformation of coral skeletons to calcite is frequently observed, this being well reflected in the PI section.

The origin of the calcrete that caps the Al-Hajaja terrace is more pedogenic because it is more surficial and occurs in the vadose zone. Being a mainland terrace, it receives a continuous fluvial/alluvial sediment supply from the continental area.

Rhizoliths (vegetation roots) are rare, which indicates that arid to hyper-arid climatic conditions prevailed in the area most of the time.

An increase in rainfall as a result of intensified Indian summer monsoons during the transition from interglacial to glacial periods was associated with a terrigenous input, predominantly aeolian, transported from Northern Africa and/or from the Arabian Peninsula into the southern Red Sea region before getting precipitated during the dry period to form calcrete deposits ([55] and references therein).

An arid to semi-arid environment favours calcrete formation, and a soil moisture deficit is required to allow carbonate to accumulate [96]. Since a wet climate is a prerequisite to mobilize the carbonate before it gets precipitated during the dry period, the current dry climate that prevails in the Red Sea region is less conducive for calcrete to develop. The only conducive period was during the wet periods in Arabia, concomitant with an increase in precipitation seasonality relative to the dry seasonality of glacial periods [79], [97], [98]

5.2.1 Stratigraphic correlations between different sections of Pleistocene age

Lithostratigraphic correlation of environmental facies showing successive events consequent/alternate each terrace (Figure 9). Comparison between the investigated sites in YRS indicates that each carbonate deposit of Pleistocene age can be subdivided into 2 or 3 main sequences. The upper sequence is characterized by the dominance of coral and coralline algal frameworks in all sites. However, the lower sequences are varied from site to site, based on the location and age. The differentiation between the two sequences can be attributed to the variability of climatic conditions.

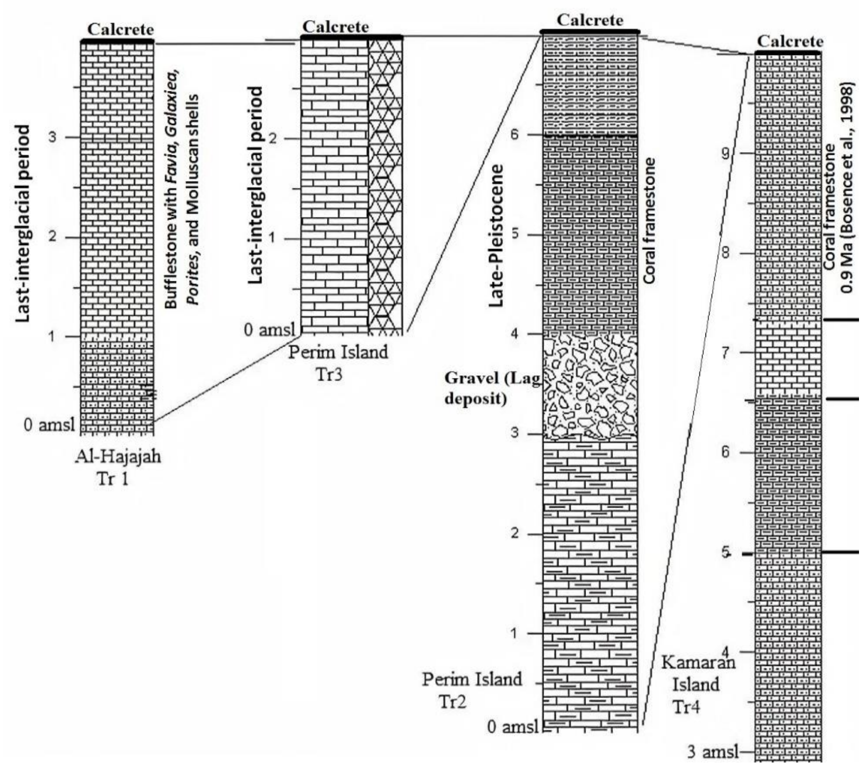

Figure 9. Comparison between sequences from YRS.

Tr1 is mainly composed of corals, grainstones, packstones, or wackestones rich in the debris of mollusks and calcareous algae. The lower section has poorly developed corals suggesting climatic conditions were not optimal for coral to grow. The presence of corals in the form of framework or isolated patches suggests a rapid increase of accommodation, and probably a reduction in terrigenous and siliciclastic inputs. The whole terrace belongs to the last interglacial period known as the Marine Isotope Stage (MIS 5e). In contrast, Tr2 terrace has gone through complex events of transgression/ regression processes that have led to a gravel deposit at the base (lag deposit), unconformably overlain by a sequence of diagenetically altered framework and patch corals set unconformably above the lag deposit, suggesting sea-level regression and transgression. Aerial to sub-aerial exposure during low sea-level stands allowed coral interaction with meteoric water that recrystallized the fossil corals, and aragonite transformed into calcite. Tr3 chiefly consists of a bioclastic framework of coral rubbles and shell fractions. The other skeletal fractions include brachiopods, gastropods, and mollusks, etc. The biological assemblages in the exposed beach rock and terrace indicate intertidal environmental conditions. Tr4 is the oldest section and the upper section is formed of coral framestone of early Pleistocene [62].

5.3 Implications for paleoclimate

The availability of adequate supplies of well-sorted beach sands and onshore winds capable of moving sand for at least part of the year is the basic requirement for the formation of coastal dunes [99]. Thus, the southwest Indian and African monsoons prevailing in southern Arabia are the main cause of coastal dune formation in the southern Red Sea. Similar to other deposits in a range of locations worldwide; e.g southern Australia [37], [38], [39], [40], [41], [42], [43], the Bahama Islands [44]; and South Africa [45], [46], oscillation during the Pleistocene time was accompanied by cyclic deposition of aeolianites across the Red Sea. The transition from interglacial to glacial climates in Arabia was characterized by higher effective rainfall, accompanied by aeolianite dissolution and karstification. The long exposure during a glacial period of coastal terraces already hosting abundant sand-sized skeletal debris of marine organisms accumulated during the previous interglacial sea-level highstands paved the way for calcretization. The glacial period of Arabia was a period of dryness and does not support carbonate sand deposition; instead laminated microbialite and/or laminar calcrete occurred.

6. Conclusion

Most of the information on the timing of wet periods in southern Arabia prior to the Holocene and human dispersal has been mainly acquired through speleothem records from the southeastern edges of the peninsula (speleothem records from far Eastern Yemen and Oman). However, information regarding hydrological patterns from the Yemeni highlands that represent the limit of the intertropical convergence zone is scarce. Calcrete deposit can form an alternative for the palaeohydrological study of south Arabia given the lack of palaeoclimatic indicators in the area. Calcrete deposits atop the coastline of the YRS are the result of dry and wet seasons corresponding to the glacial and interglacial periods during the Pleistocene time, respectively. Widespread coral diagenesis throughout the YRS terraces of the Late-Pleistocene age is another indication of influential rainfall during the Pleistocene age.

Acknowledgment

This study was supported by the U.S Fulbright Association awarded to Ahmed Al-Mikhlafi at the University of Minnesota, USA. Financial support received from the Fulbright Association during Al-Mikhlafi’s stay in the US is gratefully acknowledged. Special thanks go to Rick Knurr for assistance in XRD analysis. The guidance and comments received from Dr. Salah Al-Khirbash of SQU are highly acknowledged. I thank the anonymous reviewers for their thoughtful reviews that greatly improved the manuscript.

References

1. Davison, I., Al-Kadasi, M., Al-Khirbash, S., Al-Subbary, A., Baker, J., Blakey, S., Bosence, D., Dart, C., Heaton, R., Heaton, R., McClay, K., Menzies, M., Nichols, G., Owen, L., Yelland, A. Geological evolution of the southeastern Red Sea Rift margin, Republic of Yemen, *Geological Society of American Bulletin*.1994, **106**, 1474-1493.
2. Al-Sayari, S.S. and Zotl, J.G. Quaternary Period in Saudi Arabia 1. Sedimentological, Hydrogeological, Hydrochemical, Geomorphological, and Climatological Investigations in Central and Eastern Saudi Arabia. *Springer Verlag*, *Vienna*. 1978, http://dx.doi.org/10.1007/978-3-7091-8494-3.
3. Klaus, R. Coral reefs and communities of the central and Southern Red Sea (Sudan, Eritrea, Djiuti, and Yemen. *Plos One*. 2012, **7(5)**, 1-7.
4. Al-Mikhlafi, A.S., Edwards, R.L., Cheng, H. Sea-level history and tectonic uplift during the last-interglacial period (LIG) inferred from the Bab al-Mandab coral reef terraces, Yemen, *Journal of African Earth Science*. 2018, **138**, 133-148.
5. Turak, E., Brodie, J. Coral and reef habitats. In: DouAbul, A., Rouphael, T.S., Marchant, R. (Eds.), Ecosystems of the Red Sea Coast of Yemen, Protection of Marine Ecosystems of the Red Sea Coast of Yemen. *Hassell and Assoc., AMSAT and UNOPS*. 1999.
6. Hamed, B., Bussert, R., and Dominik, W. Stratigraphy and evolution of emerged Pleistocene reefs at the Red Sea coast of Sudan. *Journal of African Earth Sciences*. 2016, **114**, 133-142.
7. Gvirtzman, G, and Friedman, G.M. Sequence of progressive diagenesis in coral reefs. In: Frost SH, Weiss MP, Saunders JB (eds) Reefs and related carbonates: ecology and sedimentology. *American Association Petroleum Geologists.* 1977, **4**, 57-380
8. Friedman, G.M. 1968. Geology and geochemistry of reefs, carbonate sediments and waters, Gulf of Aqaba (Elat), Red Sea. *Journal of Sedimentary Petrology.* 1977, **38**, 895-919.
9. Friedman, G. M. Gulf of Elat (Aqaba). Geological and sedimentological framework. *In:* Friedman G.M. and W.E. Krumbein (Eds) Hypersaline Ecosystems. The Gavish Sabkha. *Springer Verlag, Berlin*. 1985, Chapter **3**, pp 3971.
10. E1-Asmar, H.M. and Attia, G. Diagenetic trends in Quaternary coral reef terraces, Ras Mohammed-Sharm ElSheikh coast, Southern Sinai, Egypt. *Sedimentology of Egypt*, 1996, **4**, 19-31.
11. Strasser A., Strohmenger C., Davaud E. and Bach A. Sequential evolution and diagenesis of Pleistocene coral reefs (south Sinai, Egypt). *Sedimentary Geology.* 1992, **78**, 59-79.

12. Al-Mikhlafi, A.S., Fiona, H., Edwards, R.L., Cheng, H. Holocene relative sea-level changes and coastal evolution along the coastlines of Kamaran and As-Salif Peninsula, Yemen, southern Red Sea. *Quaternary Science Review*. 2021, **252**, https://doi.org/10.1016/j.quascirev.2020.106719.
13. Allison, N., Finch, A.A., Webster, J.M. and Clague D.A. Palaeoenvironmental records from fossil corals: The effects of submarine diagenesis on temperature and climate estimates. *Geochemica et Cosmochimica. Acta* 2007. **71(19)**, 4693-4703.
14. Hendy, E.J. Gagan, M., Lough, J., McCulloch, M. and deMenoca, P. Impact of skeletal dissolution and secondary aragonite on trace element and isotopic climate proxies in Porites corals. *Paleoceanography*. 2007, **22**, 1-10.
15. Muller, A., Gagan, M.K. and McCulloch, M.T. Early marine diagenesis in coral and geochemical consequences for paleoceanographic reconstructions. *Geophysical Research Letters.* 2001, **28(23)**, 4471-4474.
16. Sayani, H.R., Cobb, K.M., Cohen, A.L., Elliott, W.C., Nurhati, I.S., Dunbar, R.B., Rose, K.A., Zaunbrecher, L.K. *Effects of diagenesis on paleoclimate reconstructions from modern and young fossil corals. Geochimica et Cosmochimica Acta*. 2011, **75(21)**, 6361-6373.
17. Murphy, R.J., Webster, J.M., Nothdurft, L., Dechnik, B., McGregor, H.V., Patterson, M.A., Sanborn, K.L., Webb, G. E., Kearney, L.I., Rintoul, L. and Erler, D.V. High-resolution hyperspectral imaging of diagenesis and clays in fossil coral reef material: a nondestructive tool for improving environmental and climate reconstructions. *G3: Geochemistry, Geophysics, Geosystems: An Electronic Journal of the Earth Sciences*. 2017, **18(8)**, 3209-3230.
18. Dechnik, B., Webster, J.M., Webb, G.E., Nothdurft, L., Zhao, J.X. Successive phases of Holocene reef flat development: evidence from the mid- to outer Great Barrier Reef. *Palaeogeography, Palaeoclimatology, Palaeoecology*. 2017, **466**, 221-230.
19. Marshall, J.F. Submarine cementation in a high-energy platform reef: One Tree Reef, southern Great Barrier Reef. *Journal of Sediment Research.* 1983, **53**, 1133-1149.
20. McGregor, H.V. and Abram, N.J. Images of diagenetic textures in Porites corals from Papua New Guinea and Indonesia. *Geochemistry, Geophysics, Geosystem.* 2008, **9**, Q10013, doi:10.1029/2008GC002093.
21. Nothdurft, L.D., Webb, G.E., Bostrom, T. and Rintoul, L. Calcite-filled borings in the most recently deposited skeleton in livecollected Porites (Scleractinia): Implications for trace element archives. *Geochimica et Cosmochimica Acta.* 2007, **71(22)**, 5423-5438.
22. Tucker, M. Sedimentary Petrology: An Introduction to the Origin of Sedimentary Rocks, 2nd ed. *Blackwell, Malden, Mass.* 1991, 260 pp.
23. Bathurst, R.G.C. Carbonate sediments and their diagenesis, 2nd Edition: *Elsevier*, *Developments in Sedimentology.* 1975, **12**, 658 p.
24. Tucker, M.E., Wright, V.P. Carbonate Sedimentology. *Blackwell Scientific Publications, Oxford*. 1990.
25. Morse, J.W. and Mackenzie, F.T. Geochemistry of Sedimentary Carbonates. *Elsevier, New York*. 1990.
26. Taviani, M., Montagna, P., Rasul, N.M.A., Angeletti, L., and Bosworth, W. Pleistocene coral reef terraces on the Saudi Arabian side of the Gulf of Aqaba, Red Sea. Eds N.M.A. Rasul and I.C.F. Stewart (eds.), Geological Setting. Palaeoenvironment and Archaeology of the Red Sea. 2019. https://doi.org/10.1007/978-3-319-99408-6_16.
27. Dullo, W-C. Facies, fossil record, and age of Pleistocene reefs from the Red Sea (Saudi Arabia). *Facies*. 1990, **22**,1-46
28. El-Sorogy, A., Youssef, M., Al-Sabrouty, M., and Al-Otaiby, N. Facies pattern and molluscan fauna of the Late Pleistocene raised coral reef of Rabigh area, Red Sea coast, Saudi Arabia. *Indian Journal of Geo-Marine Sciences.* 2014, **43**, 1571-1580.
29. Manaa, A.A., Jones, B.G., McGregor, H.V., Zhao, J., and Price, D.M. Dating Quaternary raised coral terraces along the Saudi Arabian Red Sea coast. *Marine Geology.* 2016, **374**, 59-72.
30. Khalil, H. M. Pliocene–Pleistocene stratigraphy and macrofauna of the Farasan Islands, South East Red Sea, Saudi Arabia. *Arabian Journal of Geosciences*, 2011, **5**, 1223-1245.
31. Mandurah, M.H. and Aref, M.A. Lithostratigraphy and standard microfacies types of the Neogene carbonates of Rabigh and Ubhur areas, Red Sea coastal plain of Saudi Arabia. *Arabian Journal of Geosciences*. 2012, **5**, 1317-1332.
32. Sakellariou, D., Rousakis, G., Panagiotopoulos, I., Morfis, I., Bailey, G.N. Geological Structure and Late Quaternary Geomorphological Evolution of the Farasan Islands Continental Shelf , South Red Sea, sw Saudi Arabia. *Springer International Publishing*. 2019, https://doi.org/10.1007/978-3-319-99408-6.

33. Angelucci, A., Matteucci, R., Praturlon, A. Outline of geology and sedimentary environments of the Dahlak Islands (southern Red Sea). *Bollettino della Societs Geologica Italiana.* 1981, **99**, 405-419.
34. Bruggemann, J.H., Buffler, R.T., Guillaume, M.M.M., Walter, R.C., von Cosel, R., Ghebretensae, B.N., Berhe, S.M. Stratigraphy, palaeoenvironments and model for the deposition of the Abdur Reef Limestone: context for an important archaeological site from the last interglacial on the Red Sea coast of Eritrea. *Palaeogeography, Palaeoclimatology, Palaeoecology*. 2004, **203**, 179-206.
35. Barratt, L., Dawson-Shepherd, A., Ormond, R.F.G., McDowall, R. Former Yemen Arab Republic marine conservation survey. vol. I. Distribution of habitats and species along the YAR coastline. *IUCN Red Sea and Gulf of Aden Environment Program*/TMRU York, UK. 1987, 110, 2pp.
36. Turak, E., Brodie, J., Devantier, L. Reef-building corals and coral communities of the Yemen Red Sea: *Fauna of Arabia*. 2007, **23**, 1- 40.
37. Gardner, T., Webb, J., Davis, A., Cassel, E., Pezzia, C., Merritts, D., and Smith, B. Late Pleistocene landscape response to climate change: eolian and alluvial fan deposition, Cape Liptrap, southeastern Australia. *Quaternary Science Reviews*. 2006, **25**, 1552-1569.
38. Hearty, P.J. and O'Leary, M.J. Carbonate aeolianites, quartz sands, and Quaternary sea- level cycles, Western Australia: a chronostratigraphic approach. *Quaternary Geochronology.* 2008, **3**, 26-55.
39. Murray-Wallace, C.V., Bourman, R.P., Prescott, J.R., Williams, F., Price, D.M. and Belperio, A.P. Aminostratigraphy and thermoluminescence dating of coastal aeolianites and the later Quaternary history of a failed delta: the River Murray mouth region, South Australia. *Quaternary Geochronology*. 2010, **5**, 28-49.
40. Lomax, J., Hilgers, A., Radtke, U. Palaeoenvironmental change recorded in the palaeodunefields of the western Murray Basin, South Australia – new data from single OSL-dating. *Quaternary Science Review*. 2011, **30**, 723-736.
41. Playford, P.E., Cockbain, A.E., Berry, P.F., Roberts, A.P., Haines, P.W. and Brooke, B.P. The Geology of Shark Bay. *Geological Survey of Western Australia Bulletin*. 2013, **146**, 281.
42. Brooke, B.P., Olley, J.M., Pietsch, T., Playford, P.E., Haines, P.W., Murray-Wallace, C.V., Woodroffe, C.D. Chronology of Quaternary coastal aeolianite deposition and the drowned shorelines of southwestern Western Australia – a reappraisal. *Quaternary Science Review*. 2014, **93**, 106-124.
43. Lipar, M., Webb, J.A., Cupper, M.L., and Wang, N. Aeolianite, calcrete/microbialite and karst in Southwestern Australia as indicators of Middle to Late Quaternary Palaeoclimates. *Palaeogeography, Palaeoclimatology, Palaeoecology*. 2017, **470**, 11-29.
44. Mylroie, J.E. Late-Quaternary sea-level position: evidence from Bahamian carbonate deposition and dissolution cycles. *Quaternary International*. 2008, **183**, 61-75.
45. Porat, N. and Botha, G. The luminescence chronology of dune development on the Maputaland coastal plain, southeast Africa. *Quaternary Science Review.* 2008, **27**, 1024-1046.
46. Bateman, M.D., Carr, A.S., Dunajko, A.C., Holmes, P.J., Roberts, D.L., Mclaren, S., Bryant, R.G., Marker, M.E., Murray-Wallace, C.V. The evolution of coastal barrier systems: a case study of the Middle-Late Pleistocene Wilderness barriers, South Africa. *Quaternary Science Review.* 2011, **30**, 63-81.
47. Van Campo, E.,. Duplessy, J.C and Rossignol-Strick, M. Climatic conditions deduced from a 150-kyr oxygen isotope-pollen record from the Arabian Sea. *Nature*, 1982, **296**, 56-59.
48. Clemens, S.C., and Prell W.L. Late Pleistocene variability of Arabian summer monsoon winds and continental aridity: Eolian records from the lithogenic component of deep-sea sediments. *Paleoceanography*. 1990, **5**, 109-145.
49. deMenocal, P.B. African climate change and faunal evolution during the Pliocene-Pleistocene. *Earth and Planetary Science Letters*. 1990, **220(1-2)**, 3-24.
50. Kolla, V., L. Henderson, and P. Biscaye. Clay mineralogy and sedimentation in the Western Indian Ocean. *Deep Sea Reseach and Oceanographic abstracts*. 1976, **23**, 949-961.
51. Leuschner, D.C., and Sirocko, F. The low-latitude monsoon climate during Dansgaard-Oeschger cycles and Heinrich Events. *Quaternary Science Reviews*. 2000, **19(1-5)**, 243-254.
52. Sirocko, F., and Lange, H. Clay mineral accumulation rates in the Arabian Sea during the Late Quaternary. *Marine Geology*. 1991, **97**, 105-119.
53. Sirocko, F., Sarnthein, M., Erlenkeuser, H., Lange, H., Arnold, M. and J. C. Duplessy. Century-scale events in monsoonal climate over the past 24,000 years. *Nature*, 1991, **364**, 322-324.
54. Sirocko, F., Garbe-Schönberg, D. and Devey, C. Processes controlling trace element geochemistry of Arabian Sea sediments during the last 25,000 years. *Global Planet Change.* 2000, **26**, 217-303.

55. Bouilloux, A., Valet, J.-P., Bassinot, F., Joron, J.L., Dewilde, F., Blanc-Valleron M.-M., Moreno, E. Influence of seawater exchanges across the Bab-el-Mandeb Strait on sedimentation in the Southern Red Sea during the last 60 ka. *Paleoceanography.* 2013, **28**, 675-687.
56. Isaji, Y., Kawahata, H., Ohkouchi, N., Murayama, M. and Tamaki, K. Terrestrial environmental changes around the Gulf of Aden over the last 210 kyr deduced from the sediment n-alkane record: Implications for the dispersal of Homo sapiens. *Geophysical Research Letters.* 2015, **42**, 1880-1887.
57. Beydoun, Z.R., As-Saruri, M.L., El-Nakhak, H., Al-Ganad., I.N., Baraba, R.S., Nani, A.O., and Al-Aawah, M.H. International lexicon of stratigraphy, Republic of Yemen: Vol. III, *Asia*, *fascicule*, 10b2. *IUGS Publication*. 1988, **34**, 245pp.
58. Purkis, S.J., Harris, P. M., Ellis, J. Patterns of sedimentation in the contemporary red sea as an analog for ancient carbonates in rift settings. *Journal of Sedimentary Research.* 2012, **82(11),** 859-870.
59. Meteorological and Environmental Protection Administration (MEPA)/ International Union for Conversation of Nature (IUCN). Saudi Arabia: assessment of coastal zone management requirements. *MEPA. Published report* 1987, **7**, Jeddah.
60. Sheppard, C., Price, A., and Roberts, C. Marine ecology of the Arabian region: patterns and processes in extreme tropical environments. *Academic Press, London*. 1992.
61. Dullo, W.C., Montaggioni, L. Modern Red Sea coral reefs: a review of their morphologies and zonation. In: Purser BH, Bosence DWJ (eds) Sedimentation and tectonics of rift basins: Red Sea-Gulf of Aden. *Chapman and Hall, London.* 1998, 583-594.
62. Bosence, D.W.J., Al-Aawah, M.H., Davidson I, Rosen, B., Vita-Finzi, C., Whittaker, L. Salt domes and their control on basin margin sedimentation: a case study from Tihama Plain, Yemen. In: Purser BH, Bosence DWJ (eds) Sedimentation and tectonics of rift basins: Red Sea-Gulf of Aden. *Chapman and Hall, London*. 1998, pp 450-467.
63. Rowlands, G. and Purkis, S. Geomorphology of shallow water coral reef environments in the Red Sea. In: Rasul, N.M.A., Stewart, I.C.F. (Eds.), the Red Sea, Springer Earth System Sciences. *Springer-Verlag Berlin Heidelberg*. 2015.
64. Lambeck, K., Purcell, A., Flemming, N.C., Vita-Finzi, C., Alsharekh, A.M., Bailey G.N. Sea-level and shoreline reconstructions for the Red Sea: isostatic and tectonic considerations and implications for hominin migration out of Africa. *Quaternary Science Review*. 2011, **30**, 3542-3574.
65. Montaggioni, L.F. and Faure, G. Response of reef coral communities to sea-level rise: a Holocene model from Mauritius (western Indian Ocean). *Sedimentology.* 1997, **44**, 1053-1070.
66. Gvirtzman, G., Buchbinder, B., Shen, A., Nir, Y., and Friedman, G.M. Morphology of the Red Sea fringing reefs a result of the erosional pattern of the last-glacial low-stand sea level and the following Holocene recolonization. *Bureau Recherches Ge´ologiques et Minie`res (France), Me´moires*. 1977, **89**, 480-491.
67. Edgell, H.S. Coastal Deserts of Arabia in Springer book, Arabian Deserts, nature, origin, and evolution. *Springer*. 2006, 385.
68. Tosi, M. Survey and Excavations on the Coastal Plain (Tihamah). *East and West*. 1986, **36**, 400-414.
69. Jarosz, E., Murray, S.P., and Inoue, M. Observations on the characteristics of tides in the Bab el Mandab Strait. *Journal of Geophysical Research*. 2005, 110, C03015.
70. Thornborough and Davies. Reef Flats in Hopley, D. Editor. *Encyclopedia of Modern Coral Reefs*. 2011, pp. 869-876.
71. Almalki, K.A., Bantan, R.A. Lithologic units and stratigraphy of the Farasan Islands, Southern Red Sea. *Carbonates and Evaporites*. 2016, **31**, 115-128.
72. Whittle, L.G., Kendall, C.G., Dill, R.F., and Rouch, L. Carbonate cement fabrics displayed: a transverse across the margin of the Bahamas platforms near Lee Stocking in the Exuma cays. *Marine Geology*. 1993, **110**, 213-243.
73. Cramer, M.D., Hawkins, H.J. A physiological mechanism for the formation of root casts. *Palaeogeography, Palaeoclimatology, Palaeoecology*. 2009, **274**, 125-133.
74. Klappa, C.F. Rhizoliths in terrestrial carbonates: classification, recognition, genesis and significance. *Sedimentology*. 1980, **27**, 613-629.
75. Nash, M.C., Opdyke, B.N., Wu, Z. and Xu, H. Simple X-Ray diffraction techniques to identify MG calcite, dolomite, and magnesite In Tropical Coralline Algae and Assess Peak Asymmetry. *Journal of Sedimentary Research*. 2013, **83**, 1084-1098.
76. Nabhan, A. I. Holocene sedimentology and stratigraphy of coastal sediments in an arid climate, Al Qahmah, Southern Red Sea, Saudi Arabia, Ph.D. thesis. *Missouri University of Science and Technology*. 2015. https://scholarsmine.mst.edu/doctoral_dissertations/2454.

77. Kennedy, D.M. and Woodroffe, C. Fringing reef growth and morphology: *A review*. *Earth-Science Reviews*. 2002, **57(3)**, 255-277.
78. Davies, C.P. Holocene paleoclimaes of southern Arabia from lacustrine deposits of the Dhamar highlands, Yemen. *Quaternary Research*, 2006, **66**, 454-464.
79. Fleitmann, D., Burns, S.J., Pekala, M., Mangini, A., Al-Subbary, A., Al-Aowah, M., Kramers, J., and Matter, A. Holocene and Pleistocene pluvial periods in Yemen, southern Arabia. *Quaternary Science Reviews*. 2011, **30**, 783-787.
80. Burns, S.J., Fleitmann, D., Matter, A., Kramers, J., Al-Subbary, A. Indian Ocean climate and an absolute chronology over Dansgaard/Oeschger events 9-13. *Science*. 2003, **301**. 1365-1367.
81. Fleitmann, D., and Matter, A. The speleothem record of climate variability in Southern Arabian. *Geosciences*. 2009, **341**, 633-642.
82. Lazar B, Stein M. Freshwater on the route of hominids out of Africa revealed by U-Th in Red Sea corals. *Geological Society of America*. 2011, **39**. 1067-1070.
83. Nicholson, S.L., Pike, AWG, Hosfield, R., Roberts, N, Sahy, D., woodhead, J., Cheng, H., Lawrence Edwards, R., Affolter, Stephane, Leuenberger, M., Burns, S.J, Matter, A., Fleitmann, D. Pluvial periods in southern Arabia over the last 1.1 million-years. *Quaternary Science Review*. 2020, 106112.
84. Badiozamani, K. The Dorag Dolomitization Model, Application to the Middle Ordovician of Wisconsin. *Journal of Sedimentary Research*. 1973, **43**, 965-984.
85. Humphrey, J.D. Late Pleistocene Mixing Zone Dolomitization, South-Eastern Barbados, West Indies. *Sedimentology*. 1988, **35**, 327-348.
86. Sherman, C.E., Fletcher III, C.H., and Rubin, K.H. Marine and meteoric diagenesis of Pleistocene carbonates from a nearshore submarine terrace, Oahu, Hawaii. *Journal of Sedimentary Research*. 1999, **69**, 1083–1097.
87. James, N. P. Diagenesis of scleractinian corals in subaerial vadose environment. *Journal of Paleontology*. 1974, **48**, 785-799.
88. Deffeyes, K.S., Lucia, F.J. and Weyl, P.K. Dolomitization of recent and Plio-Pleistocene sediments by marine evaporite waters on Bonaire, Netherlands Antilles. In: L.C. Pray and R.C. Murray (Editors), Dolomitization and Limestone Diagenesis. *Society of Economic Paleontologists and Mineralogists. Special Publication.* 1965, **13**, 71-88.
89. Lucia, E.J., and Majdr, R.P. Porosity evolution through hypersaline reflux dolomitization. In: PURSER, B.H., TUCKER M.E. and ZENGER, D.H. (eds) Dolomites - A Volume in Honour of Dolomieu. *International Association of Sedimentologists, Special Publications*. 1994, **21**, 325-341.
90. Rodrigues, A.G, Fernando, Ros, L.D., Neumann, R. and Borghi, L. Paleoenvironmental implications of early diagenetic siderites of the Paraíba do Sul Deltaic Complex, eastern Brazil. *Sedimentary Geology*. 2015, **323**, 15-30.
91. Berner, R.A. A new geochemical classification of sedimentary environments. *Journal of Sedimentary Petrology*. 1981, **51**, 359-365.
92. Coleman, M.L. Geochemistry of diagenetic non-silicate minerals: kinetic considerations. *Philosophical Transactions of the Royal Society of London Series A, Mathematical and Physical Sciences*. 1985, **315**, 39-56.
93. Berner, R.A. Principles of Sedimentology. *McGraw-Hill, New York*. 1971, 240pp.
94. Maynard, J.B. Extension of Berner's “new geochemical classification of sedimentary environments” to ancient sediments. *Journal of Sedimentary Petrology*. 1982, **52**, 1325-1331.
95. Pye, K., Dickson, J.A.D, Schiavon, N., Coleman, M.L. and Cox, M. Formation of Siderite-Mg calcite-iron sulfide concretions in intertidal marsh and sandflat sediments, north Norfolk, England. *Sedimentology*. 1990, **37**, 325-343.
96. Wright, V.P. Paleosols in shallow marine carbonate sequences. *Earth Science Reviews*. 1994, **35**, 367-395.
97. Fleitmann, D., Burns, S.J., Mudelsee, M., Neff, U., Kramers J, Mangini, A. Holocene forcing of the Indian monsoon recorded in a stalactite from Southern Oman. *Science*. 2003, **300**, 1737-1739.
98. Fleitmann, D., Burns, S.J., Mangini, A., Mudelsee, M., Kramers, J., Villa, I., Neff, U., Al-Subbary, A.A., Buettner, A., Hippler, D., and Matter, A. Holocene ITCZ and Indian monsoon dynamics recorded in stalagmites from Oman and Yemen (Socotra). *Quaternary Science Reviews*. 2007, **26**, 170-188.
99. Pye, K. Coastal Dunes. *Progress in Physical Geography*. 1983, **7**, 531.

Received 22 September 2020
Accepted 4 February 2021